Acta Materialia 142 (2018) 82–94

Contents lists available at ScienceDirect

Acta Materialia

journal homepage: www.elsevier.com/locate/actamat

Full length article

Hot cracking mechanism affecting a non-weldable Ni-based superalloy produced by selective electron Beam Melting

Edouard Chauvet [a], Paraskevas Kontis [b], Eric A. Jägle [b], Baptiste Gault [b], Dierk Raabe [b], Catherine Tassin [a], Jean-Jacques Blandin [a], Rémy Dendievel [a], Benjamin Vayre [c], Stéphane Abed [c], Guilhem Martin [a], *

[a] Univ. Grenoble Alpes, CNRS, Grenoble INP, SIMaP, F-38000, Grenoble, France
[b] Max-Planck-Institut für Eisenforschung GmbH, Max-Planck-Strasse 1, 40237 Düsseldorf, Germany
[c] Poly-Shape, 235 Rue des Canesteu -ZI La Gandonne, 13300, Salon-de-Provence, France

ARTICLE INFO

Article history:
Received 7 June 2017
Received in revised form
20 September 2017
Accepted 21 September 2017
Available online 25 September 2017

Keywords:
Electron Beam Melting
Ni-based superalloys
Hot cracking
Grain boundaries
Liquid film
Micro-segregations

ABSTRACT

A non weldable nickel-based superalloy was fabricated by powder bed-based selective electron beam melting (S-EBM). The as-built samples exhibit a heterogeneous microstructure along the build direction. A gradient of columnar grain size as well as a significant gradient in the γ' precipitate size were found along the build direction. Microstructural defects such as gas porosity inherited from the powders, shrinkage pores and cracks inherited from the S-EBM process were identified. The origins of those defects are discussed with a particular emphasis on crack formation. Cracks were consistently found to propagate intergranular and the effect of crystallographic misorientation on the cracking behavior was investigated. A clear correlation was identified between cracks and high angle grain boundaries (HAGB). The cracks were classified as hot cracks based on the observation of the fracture surface of micro-tensile specimens machined from as-built S-EBM samples. The conditions required to trigger hot cracking, namely, presence of a liquid film during the last stage of solidification and thermal stresses are discussed within the framework of additive manufacturing. Understanding the cracking mechanism enables to provide guidelines to obtain crack-free specimens of non-weldable Ni-based superalloys produced by S-EBM.

1. Introduction

Precipitation strengthened Ni-based superalloys have been one of the great breakthroughs in materials science enabling the development of advanced and fuel efficient aero engines. Since the 1950s, this class of superalloys is in continuous development to achieve better creep and oxidation resistance, lower fatigue crack growth rate and high yield stress for service temperatures up to 1000 °C. These superalloys are typically strengthened by ordered, coherent intermetallic precipitates such as γ'-$Ni_3(Al,Ti)$ or γ''-Ni_3Nb. Different processes can be used to produce parts made of this class of Ni-based superalloys: casting [1], directional solidification [2–7], and powder metallurgy [8–10]. With the recent development of new processing and advanced manufacturing routes, in particular additive manufacturing, there is an increasing demand for producing high-temperature components made of such Ni-base superalloys. Key drivers for this include the ability to produce complex netshape components without the restrictions of traditional machining, thereby enabling optimized cooling channels that allow for higher service temperatures as well as the ability to rapidly produce small batches of complex parts without the prohibitive costs and lead times of traditional casting techniques.

Until recently, the community strongly focused on the well-known alloy Inconel 718, see e.g. Refs. [11–16], as it can be quite efficiently produced by additive manufacturing without producing critical defects. Wide processing windows have been identified for the two powder bed-based techniques selective laser melting process (SLM) [13,16] and S-EBM [12,17]. This is not surprising as Inconel 718 is usually considered to be a weldable superalloy due to its low content of γ' forming elements (Al and Ti) [18], instead relying on γ''-Ni_3Nb as strengthening precipitate phase. However, to achieve higher creep resistance under high load, superalloys

* Corresponding author.
E-mail address: guilhem.martin@simap.grenoble-inp.fr (G. Martin).

https://doi.org/10.1016/j.actamat.2017.09.047
1359-6454/

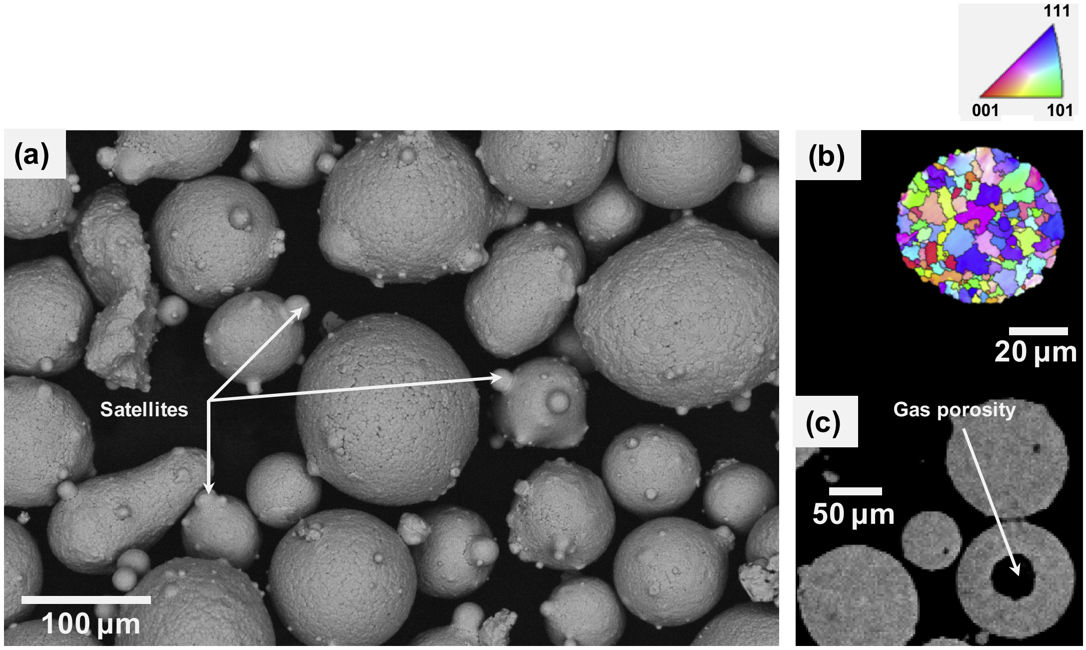

Fig. 1. Powder characteristics: (a) typical powder morphology as-revealed by SEM under secondary electron contrast (SE); (b) IPF-EBSD map revealing that the powder particles are polycrystalline; (c) SE–SEM micrograph illustrating gas porosity within initial powder particles.

with between 40 and 80% volume fraction of γ' are required. Such superalloys include Inconel 738 [19,20], CMSX-4 [21,22], René 142 [23] or CM247LC [24], which have hence recently attracted attention for usage in additive manufacturing processes. Those alloys contain comparatively high contents of Al and Ti, are classified as non-weldable, and, as a result, are prone to cracking and hence turn out to be very challenging to produce defect free by additive manufacturing [20,24–27].

Different mechanisms have been suggested in the welding literature to explain the observed cracking tendency [18]: solidification cracking [2] and liquation cracking [28] that require the presence of liquid, or strain-age cracking [18] and ductility-dip cracking [18] that occur at the solid state.

The objective of the present work is to elucidate the mechanism and the origin of cracking in a non-weldable Ni-based superalloy fabricated by S-EBM. Using detailed microstructural characterization, combining techniques such as electron microscopy, electron backscattered diffraction and atom probe tomography, we identify a number of common features that provide insights into the origin of the cracks and discuss those in light of the models generally accepted for hot cracking in conventional processing routes.

2. Experimental procedures

2.1. Powder characteristics

The prealloyed powders were produced using vacuum induction melting (VIM) gas-atomization with Ar and provided by ERASTEEL (Spain). The material under investigation is a non weldable Ni–Co–Cr–Mo–Al–Ti–B nickel-based superalloy containing significant amounts of Cr, Co and Mo and with Ti + Al wt.% = 8.6. The exact chemical composition of the atomized powder cannot be indicated for industrial confidentiality reasons. The as-received powder morphology and microstructure were characterized using a Zeiss Ultra field emission gun scanning electron microscope (FEG-SEM). The as-received powders mostly exhibit a spherical morphology with a few irregular particles and a relatively high density of satellites, see Fig. 1a. Every powder particle is polycrystalline as revealed by the inverse pole figure electron backscattered diffraction map (IPF-EBSD) shown in Fig. 1b. Some of the particles contain spherical pores corresponding to entrapped gas during the atomization process (Fig. 1c). The powder size distribution was determined by laser granulometry (MALVERN Mastersize 3000), giving an average powder particle size of approximately ~75 µm. The flowability and relative powder density were measured based respectively on the Metal Powders Industry Federation standards 3 and 4. The powder bed relative density was measured to be 53.6% and a flow time of 16.0 ± 0.1 s was found for 50 g of powders going through a 2.54 mm diameter orifice (Hall flowmeter).

2.2. Sample manufacturing

The as-received prealloyed powders were loaded into an ARCAM A1 Electron Beam Melting (S-EBM) machine operating at 60 kV accelerating voltage under a controlled pressure of He set to 2.10^{-3} mbar. The powder was deposited by layers of 50 µm on a stainless steel plate (XY-plane), then slightly consolidated with a widely defocused beam and finally selectively melted using the automatic mode according to the input CAD geometry. The powder bed was slightly consolidated during the preheating stage in order to improve the mechanical behavior and electrical conductivity. This preheating stage turns out to be the key parameter to achieve a stable process: a smoke-free[1] processing windows as well as a degree of consolidation that further enables easy removal of the powder at the end of the fabrication. A suitable temperature for preheating is therefore a temperature that roughly corresponds to the first stage of sintering, i.e. formation of necks between particles without densification. Here, the preheating temperature was

[1] Smoke is defined as the phenomenon occurring when electrostatic repulsive forces between negatively charged powder particles becomes significant leading to powder particle splashing.